Utilization of geothermal waste as a silica adsorbent for biodiesel purification

by Silviana Silviana

Submission date: 01-Jul-2021 10:14PM (UTC+0700)
Submission ID: 1614590558
File name: turnitin_3_rd_proof_ok_final.pdf (3.48M)
Word count: 8407
Character count: 40852

AUTHOR'S PROOF

Korean J. Chem. Eng.
DOI: 10.1007/s11814-021-0827-z

pISSN: 0256-1115
eISSN: 1975-7220

Utilization of geothermal waste as a silica adsorbent for biodiesel purification

Silviana Silviana†, Didi Dwi Anggoro, Cantika Aulia Salsabila, and Kevin Aprilio

Department of Chemical Engineering, Faculty of Engineering, Diponegoro University,
Jl. Prof. Sudarto, SH., Kampus Tembalang Semarang 50275, Indonesia
(*Received 7 December 2020 • Revised 5 April 2021 • Accepted 29 April 2021*)

Abstract–The purification process of biodiesel requires an adsorbent to reduce glycerin content releasing high purity of biodiesel. The adsorbent must be affordable in source and process, readily available, and have high adsorption capacity. This paper discusses utilization of silica aerogel from geothermal waste as an adsorbent of biodiesel to reduce glycerin. The paper investigates the potential of a high silica content of geothermal waste as silica adsorbent by observation of the glycerin adsorption capacity and its kinetics study. At the beginning, geothermal silica preparation was subjected to the purification of geothermal silica waste using sulfuric acid, sol-gel process, and drying process at ambient pressure. This research was statistically carried out by varying the volume ratio of HCl to sodium silicate (3-5), drying time (1-2 hours), and percent weight of silica (3-5%-w) using Design-Expert® Version 8.0.6 (State-Ease, Inc). The silica product was characterized through BET, FTIR, XRF, and XRD analysis. Analysis of untreated and treated biodiesel used GPC, GCMS, and titration based on Indonesian National Standard (SNI) of No. 06-1564-1995. The optimum conditions for preparation for removing glycerin in biodiesel was reached at ratio volume of HCl to sodium silicate of 3 : 1, 2 hours of drying time, and 3%-w silica adsorbent. The optimum of surface area of the s ilica adsorbent and the glycerin adsorption capacity can be attained at 371 m^2/g glycerin and 10±0.1 mg/g, respectively. Further meaning, the glycerin concentration in biodiesel can be reduced from (4±0.10)% to (0.1±0.01)% b using the silica adsorbent performing biodiesel characterization according to SNI in terms of glycerin content. The second-order pseudo model can be used to describe the glycerin adsorption in biodiesel by determination of k at 0.0036 g/mg min at the optimum condition preparation.

Keywords: Silica Aerogel, Geothermal Waste, Glycerin Adsorption, Kinetic Study, Adsorption Rate Constants

INTRODUCTION

Energy demand considers to be dominated by fossil fuels at around 80% [1]. According to data from Secretariat General of Indonesian Ministry of Energy and Mineral Resources 2019, domestic petroleum production decreased around 18% over the last 10 years. Therefore, the Government of Indonesia declared Government Regulation number of 79 in 2014 regard to the National Energy Policy (NEP) to develop alternative energy sources. There are several current studies focusing on alternative fuel for diesel engines. The alternative energy diversification is denoted as biogas [2], bioethanol [3], and biodiesel [4].

Biodiesel can help in achieving environmental sustainability. Biodiesel reduced the exhaust emissions of carbon monoxide, hydrocarbon, and smoke intensity by 81%, 30%, and 26%. NO_x emissions decreased on an average of 9% at all engine speed when compared to euro diesel [5]. Therefore, biodiesel can be reflected as considerable interest in terms of environment friendliness. Biodiesel can be produced by mixing long chain fatty acids from vegetable oil [6], animal fat [7], used cooking oil [8], food waste leachate [9], mixture of *Rhizopus oryzae* and *Candida rugosa* lipases [10], microalgae [11], Jatropha curcas, Pungamia pinnata, soya bean, sunflower [12] with different kind of catalyst: homogeneous [13], heterogeneous [13], and enzyme [14]. Several methods of the biodiesel production have been commonly prepared by ultrasonic irradiation, microwave, batch process, and supercritical process several [15]. Among these, transesterification is affirmed as the cost-effective method widely used for biodiesel production [12].

The presence of excess impurities, such as methanol, catalyst, and glycerin, affects the quality of biodiesel [16]. The presence of water in biodiesel can promote corrosion, trigger bacterial growth, and reduce combustion heat. The presence of methanol residual in biodiesel reduces flash points, viscosity, and density. The presence of catalyst may damage the injector. While, from the presence of glycerin in biodiesel can appear problems in storage by formation of deposits in the nozzle and tank, and increase of aldehyde emissions [17]. Therefore, biodiesel product must comply with SNI (Indonesian National Standard) 7182:2015, ASTM D 6751, and EN 14214. The standard specification for biodiesel fuel can be listed such as minimum methyl ester content of 96.5%-w, maximum total glycerin of 0.24%-w, and maximum water of 0.05%-w.

Biodiesel purification is divided into two methods: dry and wet. Wet method involves hot water-washing [18] to dissolve the contaminants. However, the water releases emulsion formation such as soap which cannot dissolve free fatty acids. The biodiesel then acquires low quality. In addition, aqueous effluent from wet method can induce a detrimental environmental impact [19]. Contrary to wet method, the dry method was developed using ion exchange

†To whom correspondence should be addressed.
E-mail: silviana@che.undip.ac.id, silviana@live.undip.ac.id
Copyright by The Korean Institute of Chemical Engineers.

resin [20] and adsorbent treatment. The adsorbents in dry method are several types such as commercial magnesium silicate (Magnesol) [21,22]. However, the application of Magnesol at industrial level is still restricted by high cost [23]. Therefore, alternative adsorbents have been investigated, such as starch [24], cellulosic [24,25], rice husk ash, cow dung ash [15], and silica, such as fumed silica [26]. Adsorbent for biodiesel purification have been investigated using natural adsorbent derived from cellulose and starch from many kind of sources (maize, potato, cassava, and rice). These adsorbents release good feasibility and good efficiency in discharge impurities compared to another technique by the aqueous washing and another adsorbent of Select 450 [27]. In addition, the removal of glycerin from biodiesel using sil-ica achieved high purity of the resultant biodiesel [28,29] because glycerin has a great affinity for the silica surface [30]. Recent inves-tigations by researchers indicate the impurities removal of biodiesel can be succeed by using the silica-based waste products. [22]. Many sources of silica material can be found, such as rice husk ash [31], cow dung ash [15], chamotte clay [23], geother-mal waste [32-34]. Rice husk contains ~20% silica [31], cow dung ash contains 23.56% silica, chamotte clay contains 56.46% silica [23], geothermal waste contains 98.2% silica [33]. Therefore, geothermal waste can be used as a source of silica to produce adsorbents for biodiesel purification.

The polar substances such as glycerin can be easily attracted by basic and acidic adsorption sites of these adsorbents [15]. Glycerin has a great affinity for the silica surface [30]. It is con-sidered to modify silica to have appropriate physical properties [35- 39]. The physical properties are expected to have a large surface area to support the affinity of silica for glycerin [40-42].

The applications of silica are already broadened to many fields, such as aerospace applications, heat insulation, construction [43], adsorbent [44], membrane [45], sensor, catalyst [46], and storage media [47]. Silica has been used as an adsorbent for heavy metals such as P, Hg, and Cd [48], water vapor [49], and biodiesel [41].

Silica precursors generally used are silicon alkoxide and sodium silicate [50], alkyl-alkoxy/chloro silane (organosilane) compounds [51]. Alkoxide precursors are very expensive and carcinogenic [52]. According to economic reason, sodium silicate precursor can be used to replace the other precursors [53]. The natural resources associated with a source of silica are rice husk [22], wheat straw [54], and geothermal solid waste [55]. The geothermal plants in Dieng generate geothermal solid waste of more than 10 tons/day and contain approximately 10%-w of solids, which have been observed in many utilizations [56-60]. It is a challenge to utilize geothermal solid waste as a silica source by preparing silica aerogel as an adsorbent of biodiesel to reduce the glycerin.

This paper discusses the utilization of geothermal silica waste from geothermal plants to release sodium silica (water glass) as precursor. It resulted in the silica adsorbent for reducing the glycerin content in biodiesel by using sol-gel process and ambient pressure drying. After finding the glycerin adsorption capacity of the adsorbent, we examined the kinetic study for the adsorption. glycerin. By determination of the appropriate kinetics model, it was obtained by approaching the adsorption rate constant using pseudo-first order and pseudo-second order.

EXPERIMENTAL

1. Materials

Sulfuric acid 95-97%, sodium hydroxide 97%, ethanol 96%, $NaIO_4$ 99%, $C_2H_6O_2$ 99.5%, methanol were supplied from Merck. Hydrochloric acid 37% was purchased from Mallinckrodt. bromothymol blue was purchased from BDH Chemicals, geothermal silica waste was procured from geothermal plant in Dieng- Indonesia. Frying oil was purchased from marketplace with brand of PT Smart TbkDistillated water was provided from institution laboratory.

2. Methods

2-1. Adsorbent Preparation

Geothermal silica waste was dried at 105 °C for 24 hours [32]. Then, leaching process was conducted for 105 min at 100 °C with a ratio of 20% silica and H_2SO_4 1 : 4 w/v [57]. Afterward, the leached silica was washed using distilled water until neutral pH, then dried at 105 °C [58]. The dried silica at certain weight was contacted with 2 N NaOH for 1 hour at 95 °C to release 5%-w/w sodium silicate. Later, the impurity solid was separated from filtrate of sodium silicate. Afterward, the sodium silicate solution was mixed with 1 N HCl. The solution was then introduced aging for 12 h. The wet silica gel was washed until neutral pH [61]. The silica gel was then immersed in ethanol solution at a ratio of 1 : 3 w/v for one day. Thereafter, the silica gel was dried at 70 °C for 1-2 h, subsequently at 150 °C for 1-2 h under ambient pressure drying [62].

2-2. Production of Biodiesel

The procedure of biodiesel preparation is referred to in previous research [63]. Commercial frying oil was heated at 45 °C. Solution of KOH 5%-w/w palm oil was prepared and mixture of the oil and methanol was heated at 60 °C simultaneously with ratio of 6 mole methanol to 1 mole frying oil. Then, the KOH solution was mixed into the mixture for 1 h at 60 °C. Afterward, the solution was separated in a funnel and let stand for one day to obtain biodiesel and glycerin from the top and bottom layer glycerin of the solution, respectively.

2-3. Glycerin Adsorption Analysis and Soap Analysis

The glycerin adsorption analysis procedure adopted previous research [64]. Certain amount of the adsorbent was added into 100 ml of the biodiesel and was then stirred at 120 rpm at 30 °C for 120 minutes. The glycerin content test was carried out using titration method with triplicate determination based on Indonesian National Standard (SNI) of No. 06-1564-1995. Eight grams of biodiesel was dissolved in 10 ml of distillated water. Bromothymol blue was added as an indicator. The solution was acidified using 0.1 M H_2SO_4 until a yellow-green color. Then, the solution was neutralized using 0.05 N NaOH until forming a blue color. Afterward, 10 mL of $NaIO_4$ was added and the solution was stirred slowly. The solution was kept in a dark room at room temperature for 30 minutes. The solution was added with 2 mL of ethylene glycol and allowed to stand in a dark room at room temperature for 20 minutes. Subsequently, the solution was diluted with 60 mL of distillated water with bromothymol blue as an indicator. After that, the solution was titrated with using 0.5 N NaOH until a color of blue was attained. This procedure was also conducted for blankssolution, i.e., reagents without any samples. The glycerin content was calculated by the formula in Eq. (1) as follows (SNI 06-1564-1995):

$$GC\,(\%) = \frac{(T_1 - T_2) \times N \times 9.209}{W} \quad (1)$$

where
GC =glycerin content (%)
T_1 =volume of NaOH for sample titration (ml)
T_2 =volume of NaOH for blanks titration (ml)
N =normality of NaOH (N)
W =sample weight (gr)
9.209 =glycerin factor

The glycerin content in percent weight can be converted into dimension unit of mg/L as concentration by using Eqs. (2) and (3):

$$\text{weight of Glycerol} = GC\,(\%) \times \text{weight of Biodiesel} \quad (2)$$

$$\text{Glycerol concentration} = \frac{\text{Weight of glycerol}}{\text{Volume of biodiesel}} \quad (3)$$

Meanwhile, the soap produced during the biodiesel preparation was analyzed by using a modified version of AOCS method Cc 17-79 [65]. The sample was dissolved in 100 mL of acetone mixing with 2% of distillated water. Add 2 mL of the phenolphthalein 1% in isopropyl alcohol was added. By using titration with 0.01 N hydrochloric acid, the sample had a color change from red to clear. This required titrant was then called with A. Later, the solution was added 1 mL of bromophenol blue indicator in 4% water. The solution color changed from blue to yellow. The required titrant of hydrochloric acid was designated as B. This second titration was denoted as the amount of soap by using Eq. (4). The titration method in triplicate measurements with reliability of 90% and confidence interval of 95% resulted in soap adsorption during the glycerin adsorption.

$$\frac{B \times 0.1 \times 304.4}{1{,}000 \times W} = \text{g of soap/g of sample} \quad (4)$$

where:
B =the required hydrochloric acid in second titration (mL)
0.1 =the normality of HCl (N)
304.4 =the molecular weight of sodium oleat (g/mol)
W =the sample weight (g)

2-4. Experimental Design

The experimental was designed on statistical method using central composite design with three variables: volume ratio of HCL to sodium silicate as A with range of 3 to 5, drying time for each temperature as B at 70 °C and 150 °C (each temperature of 1 and 2 hours), and adsorbent weight of the silica as C with range of 3-5%-w. These experiments were conducted in 20 experiments with one response of q_t, i.e., glycerin adsorption capacity (Table 1). Glycerin adsorption capacity can be calculated from Eq. (5) with the glycerin concentration conversion of Eqs. (1) to (3). The responses were performed in triplicate determination by titration in order to calculate standard deviation, average, and standard error of measurement with 95% of confidence interval (CI) and reliability of 0.9 for each response data. Experimental design was used to analyze the data using Design-Expert® Version 8.0.6 (State-Ease, Inc) by using ANOVA (analysis of Variance).

Table 1. Experimental design

Run	A	B	C	q_t
1	3	2	5	5±0.10
2	3	2	3	10±0.06
3	3	1	5	5±0.03
4	5	2	3	9±0.10
5	4	1.5	4	7±0.10
6	4	1.5	2.318	12±0.10
7	5	1	5	6±0.07
8	4	1.5	5.682	5±0.09
9	4	0.66	4	7±0.20
10	5	2	5	6±0.10
11	4	1.5	4	7±0.10
12	3	1	3	10±0.10
13	4	2.341	4	7±0.10
14	4	1.5	4	7±0.10
15	4	1.5	4	7±0.09
16	5	1	3	9±0.06
17	5.682	1.5	4	7±0.10
18	4	1.5	4	7±0.335
19	2.318	1.5	4	6±0.042
20	4	1.5	4	7±0.184

A: ratio of HCl to sodium silicate (v/v)
q_t: the glycerin capacity adsorbed at time t (mg/g)
B: drying time (in hour)
C: weight percentage of the silica

The adsorbed glycerin capacity for experimental data (mg/g) was obtained by Eq. (5):

$$q = \frac{v(C_o - C_e)}{m} \quad (5)$$

where C_o denotes the initial glycerin concentration (mg/L) and C_e denotes s the glycerin concentration at equilibrium (mg/L). V reflects the volume of solution and m represents the weight of adsorbent in biodiesel purification.

2-5. Characterization

The silica was characterized in the acid leaching and in the glycerin adsorption by using XRD and FTIR, respectively. While the treated and untreated biodiesel were analyzed by GCMS. These characterizations were used to confirm the result of analysis of glycerin and soap. Furthermore, the XRD instrument was used Panalytical (Type of Expert Pro). The FTIR analysis used Shimadzu with type of IRPrestige21 by transmittance mode of acquisition. The GPC analysis used TOSOH EcoSEC Elite GPC. The BET analysis used the autosorb IQ Quantachrome Instruments from Anton Paar. The GCMS applied the GCMS type of TQ8030 from Shimadzu.

2-6. Calculation of k

The experimental data of kinetics study were analyzed using pseudo-first order and pseudo-second order [66]. The kinetics study was carried out using the adsorption test at optimum conditions of the experimental design variables, at room temperature, and stirring speed of 120 rpm. It was carried out by glycerin sampling

every 10 minutes to obtain glycerin adsorption capacity until equilibrium conditions. The experimental kinetics data were modelled using pseudo-first-order (Eq. (6)) and pseudo-second-order (Eq. (7)):

$$\log(q_e - q_t) = \log q_e - \frac{k_1}{2.303}t \quad (6)$$

where k_1 (1/min) is the adsorption rate constant in the pseudo-first order, q_e reflects is the glycerin capacity adsorbed at equilibrium and characterized by a constant glycerin concentration, and q_t (mg/g) is the glycerin capacity adsorbed at time t. By means of the slope and intercept point of $\frac{dq_t}{dt}$ versus $(q_e - q_t)$, the adsorption rate constant (k_1) can be determined.

The pseudo-second order model can be expressed by Eq. (7)

$$\frac{t}{q_t} = \frac{1}{q_e^2 k_2} + \frac{t}{q_e} \quad (7)$$

where k_2 (g/mg·min) can be determined by plotting t/q_t as the abscissa and t as the ordinate.

RESULT & DISCUSSION

1. Synthesis of Silica Aerogel

Geothermal silica waste was used as raw material to produce silica aerogel through a precursor of sodium silicate. Geothermal waste has an element content of silica up to 86.3% [33]. XRF analysis was carried out to determine the silica content in the geothermal silica waste. Based on Fig. 1, the silica content in geothermal waste was up to 80.7%.

Fig. 1 shows the results of XRF analysis. Based on the results, silica content from geothermal silica waste can be used as an adsorbent for biodiesel purification [41]. The adsorbent would be expected to have a large surface area and have good affinity for the silica surface. This properties will cause the adsorbent to be highly selective to remove glycerin in biodiesel purification [30].

However, the geothermal silica waste must be leached out of impurities such as organic and metal oxides [33]. The acid leaching process can be described with following reactions using sulfuric acid:

$$3H_2SO_{4(aq)} \rightarrow 6H^+ + 3SO_4^{2-} \quad (8)$$

$$Fe_2O_3 + 6H^+ + 3SO_4^{2-} \rightarrow Fe_2(SO_4)^3_{(aq)} + 3H_2O_{(l)} \quad (9)$$

Fig. 2 shows that silica content after leaching process increases up to 94.9% with decrease of heavy metal content. Meanwhile, XRD analysis was carried out to determine the composition of the geothermal silica waste. Fig. 3 shows the results of XRD analysis (patterns intensity against 2θ). The absence of XRD lines with high intensity shows the amorphous properties of silica. There were no other XRD lines in XRD pattern, implying that the material consisted of mostly SiO_2. Peaks 2θ at intensity of 22.5° and 22.28° show the amorphous of SiO_2 from before and after acid leaching, respectively [67]. Fig. 3 shows the geothermal silica waste is more intense after the acid leaching process. It reveals that the geothermal silica waste after leaching process has a higher silica content than that of before leaching. The XRD lines have broad peak in amorphous material due to the presence of short-range order. Meanwhile, an amorphous XRD line of leached SiO_2 was shifted to lower 2θ due to increase of thermal treatment in the sol-gel process [68].

The leached silica was then reacted with NaOH to produce so-

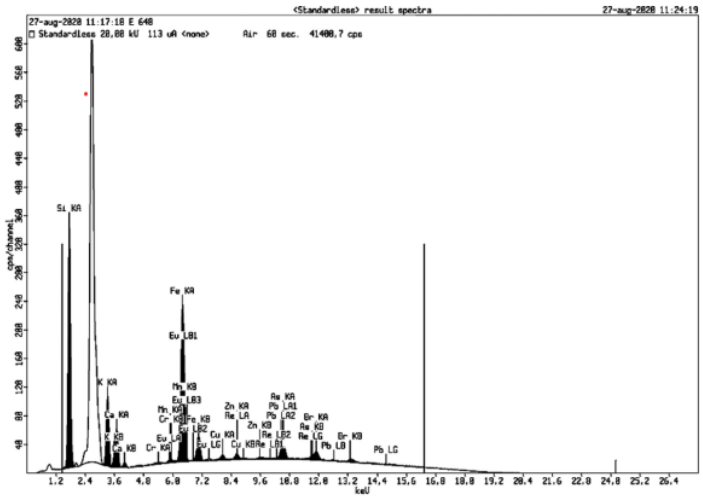

Compound	Si	K	Ca	Cr	Mn	Fe	Cu	Zn	As	Br	Eu	Re	Pb
Conc	80,7	8,37	3,63	0,079	0,07	4,82	0,15	0,14	0,69	0,57	0,3	0,2	0,3
Unit	%	%	%	%	%	%	%	%	%	%	%	%	%

Fig. 1. XRF analysis of geothermal silica waste.

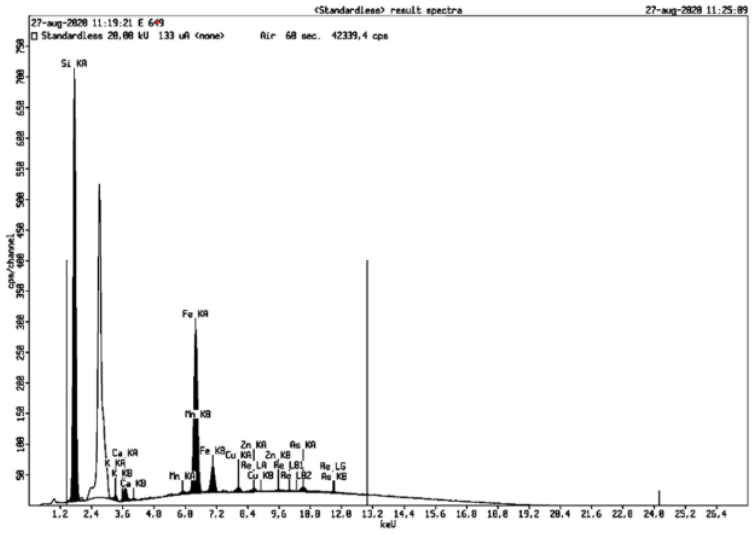

Compound	Si	K	Ca	Mn	Fe	Cu	Zn	As	Re
Conc	94,9	0,49	0,97	0,066	3,17	0,090	0,03	0,12	0,1
Unit	%	%	%	%	%	%	%	%	%

Fig. 2. XRF analysis of geothermal silica waste after leaching process.

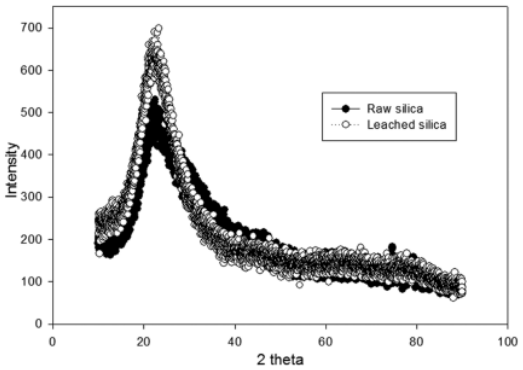

Fig. 3. XRD analysis of geothermal silica wasteand geothermal silica waste after leaching process.

dium silicate solution with the following reaction [43].

$$SiO_2+2NaOH \rightarrow Na_2O\ SiO_2+H_2O \quad (10)$$

The sodium silicate solution was added with 1 N HCl for gelation process including hydrolysis and condensation process [69]. The gelation process with HCl follows the following reaction.

$$Na_2O\ SiO_2+2HCl \rightarrow Si(OH)_4+2NaCl \quad (11)$$

The aging process was carried out by soaking the silica in ethanol after the gelation process. The aging solvent using ethanol must have a low vapor pressure to minimize silica shrinkage [43]. The pores of silica gel will contain the solvent. The aerogel properties are obtained when the solvent can be removed without any structural changes.

Based on previous research [44,70], the sol-gel process conditions such as the volume of HCl may affect the properties of silica aerogel. The drying time also affects the porosity and diameter of the silica aerogel [71]. Physical properties such as amorphous structures and large surface area can support silica in its application [54].

2. Experimental Design

This statistical method produces an equation model using Analysis of Variance (ANOVA) to determine the effect of each independent variable and the interaction between these variables on the response. Table 2 shows the analysis of variance with the quadratic model as a result.

P-value was used to determine the significance of the variable on the response. The equation model is considered significant if the p-value is less than 0.05. Table 2 shows that the p-value of the model is <0.0001; therefore, the model is significant. Table 2 also shows that variable C and the combination of AC and C^2 released a p value <0.05. Therefore, this variable has a significant effect on the q_t response. Fig. 4 shows the interaction of AC on the q_t response.

The insignificant Lack of Fit value can be seen in Table 2. The requirement for a good model shows the compatibility of the yield response data with the model.

The difference between value of predicted R^2 and adjusted R^2 is given as less than 0.2 according to Table 3. It was intended that the predicted value of the yield response data closed to the actual value. The precision value attained was around 46.2309. Further meaning, that the chosen model was feasible with of more than 4 of the precision value. An actual equation from the model as follows:

Table 2. ANOVA

Source	Sum of Squares	df	Mean square	F-value	p-Value	
Model	64.43	9	7.16	154.22	<0.0001	Significant
A-Ratio HCl	0.0339	1	0.0339	0.7303	0.4128	
B-Drying time	0.0234	1	0.0234	0.5032	0.4943	
C-Adsorbent	59.88	1	59.88	1289.97	<0.0001	
AB	0.0099	1	0.0099	0.2137	0.6538	
AC	0.3985	1	0.3985	8.58	0.0150	
BC	0.0803	1	0.0803	1.73	0.2178	
A^2	0.0028	1	0.0028	0.0610	0.8100	
B^2	0.2190	1	0.2190	4.72	0.0550	
C^2	3.85	1	3.85	83.00	<0.0001	
Residual	0.4642	10	0.0464			
Lack of fit	0.2773	5	0.0555	1.48	0.3377	Not significant
Pure error	0.1869	5	0.0374			
Cor total	64.90	19				

Sum of squares: the sum of the squared deviations from the mean due to the effect of this term
Mean square: the variance associated with that term determinated by dividing the sum of squares with the degree of fredoom.
F-value: the effect of curvature relative to the background noise.
p-Value: the probability value that is associated with F-value.

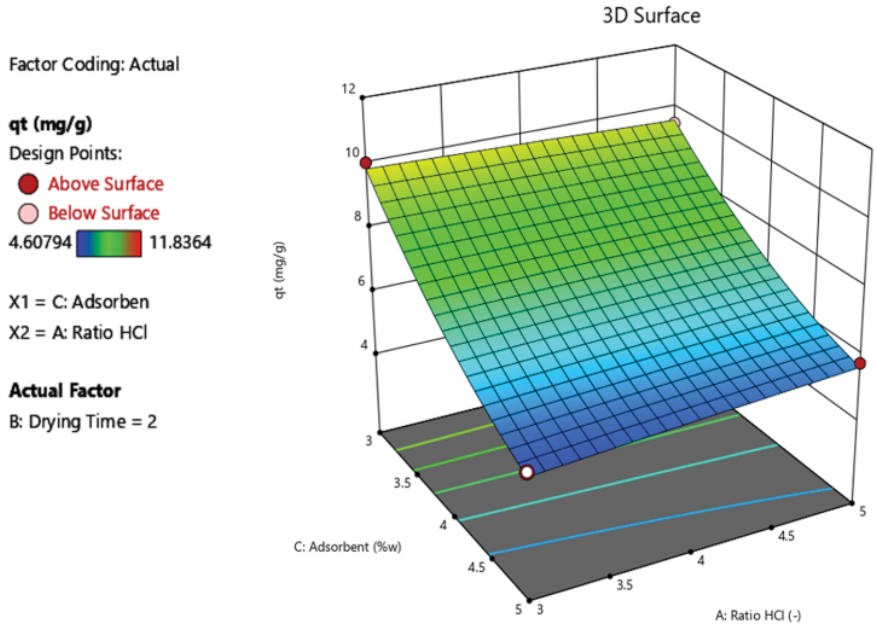

Fig. 4. Surface interaction of adsorbent weight and volume ratio HCl/sodium silicate.

$$q_t = 26{,}85140 - (0{,}836474A) - (0{,}876689B) - (6{,}82264C) + (0{,}070431AB) + (0{,}223189AC) - (0{,}223189BC) - (0{,}014013A^2) + (0{,}493046B^2) + (0{,}517057C^2) \quad (12)$$

The actual q_t can be calculated by Eq. (12). The root squared mean error (RSME) value can be determined by Eq. (13) [72]:

$$RSME = \sqrt{\frac{\sum_{i=1}^{n}(y_{prediction} - y_{experiment})^2}{n}} \quad (13)$$

The RSME value provides the error between actual and experiment. RSME value >0.5 indicates an inadequate model. This model provides RSME value <0.5 (RSME=0.15). Therefore, this model indi-

Table 3. Value of R^2

R^2	Adjusted R^2	Predicted R^2	Adeq precision
0.9928	0.9864	0.9626	46.2309

R^2: a measure of the mean variation according to the model
Adjusted R squared: R-squared adjusted for the number of parame-ters in the model relative to the number of point in the design.
Predicted R squared: the prediction measure of the model by a respon value.
Adequate precision: a range measure of predicted response with its associated error.
RMSE: Root-Square-Mean Error: the standard deviation of the residuals (prediction error)

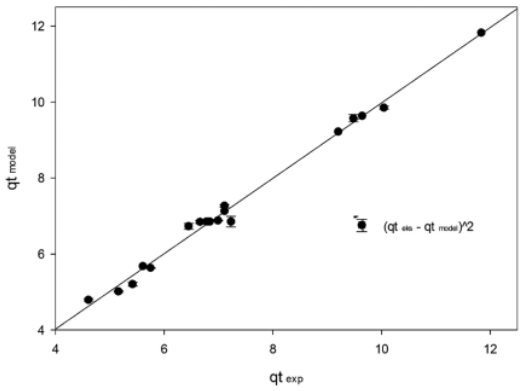

Fig. 5. q_t from the experiment and the statistical equation model for RMSE calculation.

cates an adequate predictive model. It is shown in Fig. 5.

Fig. 6 shows that the analysis of variance (ANOVA) releases equation model complying with eligibility criteria. The equation model revealed that the actual data approached the predicted data. Meanwhile, on the residual vs predicted graph, the data distribution was located within the boundary. Moreover, the optimum variables have been executed for 100 mL the biodiesel using the ratio of HCl to sodium silicate (A) at 3, drying time (B) of 2 h, 3%-w the silica adsorbent (C) releasing q_t of (10±0.061) mg/g with triplicate measurements of the glycerin analysis and reliability of 90% with 95% of confidence interval (%CI). Further meaning that the glycerin concentration of biodiesel decreased from (4±0.10)% to (0.10±0.012)% with the same condition of statistical data.

3. The Effect of HCl Volume on Surface Area of Silica Aerogel and Glycerin Adsorption Capacity

The experiment was carried out at the optimum drying condition (2 h) to determine the effect of HCl volume on the surface area. The volume ratio of HCl to sodium silicate was used in range of 3-5. Concentration of HCl affects the size, shape, specific surface area, and pore volume during the hydrolysis and polycondensation process [62]. Acid or base was used as a catalyst in hydrolysis reaction. The level of acidity influences the reaction [47]. Table 4

Table 4. Effect of the HCl ratio on the surface area of silica

Volume ratio of HCl: sodium silicate	Surface area (m^2/g)
3	371
5	109

shows the variation of the volume ratio of HCl to sodium silicate in gelation process.

Increasing the volume ratio of HCl to sodium silicate (3-5) reduced the surface area from 371 m^2/g to 108 m^2/g. The addition of HCl develops silica size to smaller due to the aggregation process on the silica aerogel microstructure [73]. Aggregation of the polymerized silicic acid during hydrolysis and condensation (gelation process) generates negative impact by reducing the mechanical properties of silica due to the limitation of the interfacial area [74]. Aggregation process can reduce the surface area of silica [75]. The effect of the HCl volume ratio on the glycerin adsorption capacity (q_t) response is visualized in Fig. 7. Decreasing volume ratio of HCl, increasing the glycerin adsorption capacity (q_t).

4. The Effect of Drying Time on Surface Area of Silica Aerogel and Glycerin Adsorption Capacity

The experiment was executed on the conditions of the volume ratio of HCl to sodium silicate at 3 to determine the effect of drying time on the surface area. It can be seen in Table 5. The porous silica as the result of hydrolysis and condensation reactions in the gelation process is acquired with Si-O-Si bonds. These bonds can trap solvent such as water or alcohol. Drying process addresses to remove the solvent from gel [47]. Ambient pressure drying was implemented in this research. Ambient pressure drying was intended with solvent evaporation and drying process at high temperature (maximum 200 °C) and atmospheric pressure. The silica aerogel preparation was statistically performed by varying the drying time (1 h and 2 h) for each temperature of 70 °C and 150 °C and constant volume ratio of HCl to sodium silicate (at 3).

Table 5 exhibits that increase of drying time could increase the surface area, i.e., 242 m^2/g to 371 m^2/g. Pore diameter of silica increases with increasing the drying time [71]. The pore contained solvent of water or alcohol would be evaporated. Therefore, the solvent can be replaced with air or CO_2 [76]. Substitution of solvent with air or CO_2 provokes the silica to become lighter with a large surface area. The evaporated solvent in the former silica gives increase of the surface area with longer drying time. The effect of drying time on the glycerin adsorption capacity (q_t) response is revealed in Fig. 8. Longer drying time increases the glycerin adsorption capacity.

5. Effect of Adsorbent Weight on Glycerin Adsorption Capacity

The effect of the adsorbent weight on the glycerin adsorption capacity glycerin was investigated during the adsorption process. The weight ratio of the silica adsorbent was applied in a range of 3%-w to 5%-w under adsorption conditions at room temperature, atmospheric pressure, and stirring speed of 120 rpm for 2 hours. Increasing amount of the adsorbent resulted in decreasing the glycerin adsorption capacity glycerin. Fig. 9 reflects that 3%-w silica has glycerin adsorption capacity up to (10±0.06) mg/g, while

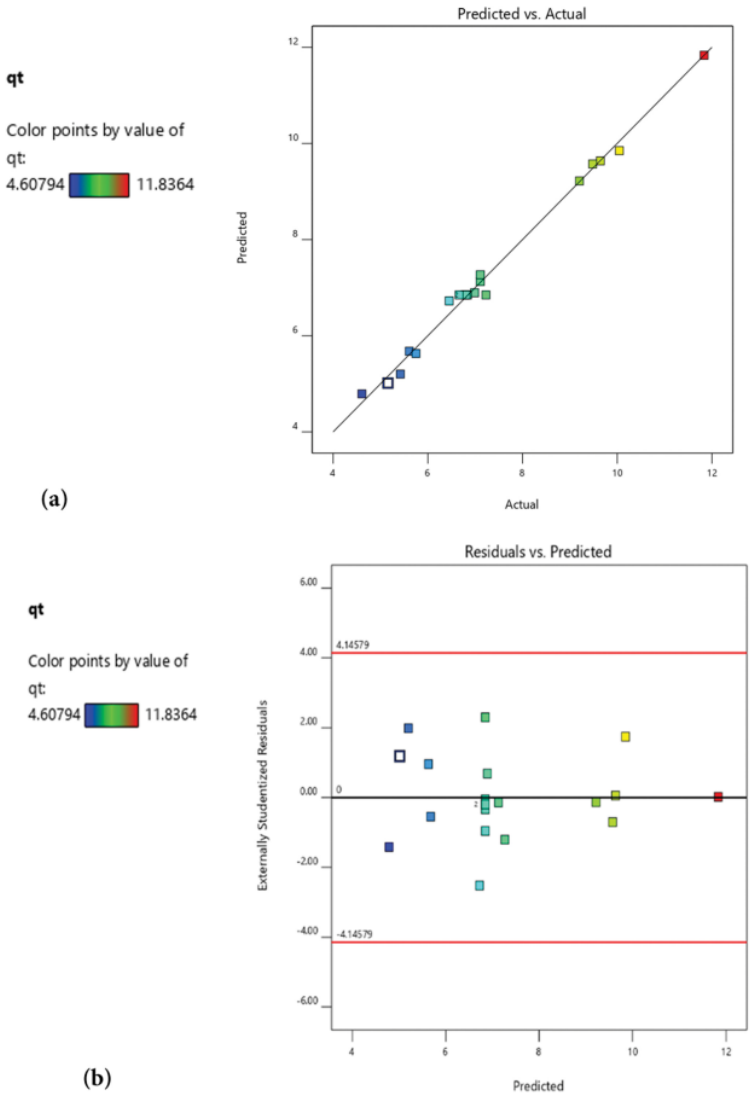

Fig. 6. Response data analysis from experiment and model (a) predicted vs actual, (b) residual vs predicted.

Table 5. Effect of drying time on the surface area of silica

Drying time (hr)	Surface area (m^2/g)
1	242
2	371

5%-w silica has glycerin adsorption capacity up to (5±0.10) mg/g. The important factor in biodiesel purification by adsorption process focuses on the unsaturated adsorbent surface [77]. Therefore, the increase of the adsorbent amount in biodiesel purification does not correspond to the increase of the glycerin adsorption capacity due to inadequate surface area of the adsorbent.

6. Characterization

The optimum condition of adsorption process in biodiesel purification was investigated by using Design-Expert® Version 8.0.6 (State-Ease, Inc). The optimum condition was reached at ratio of HCl to sodium silicate at 3, drying time of 2 h, and 3%-w silica adsorbent. The molecular weight of biodiesel used (220 g/mol) was obtained from the GPC analysis. The glycerol content of untreated biodiesel and treated biodiesel was confirmed by the GCMS analysis in Fig. 10 and Fig. 11, respectively. Fig. 10 visualizes the glyc-

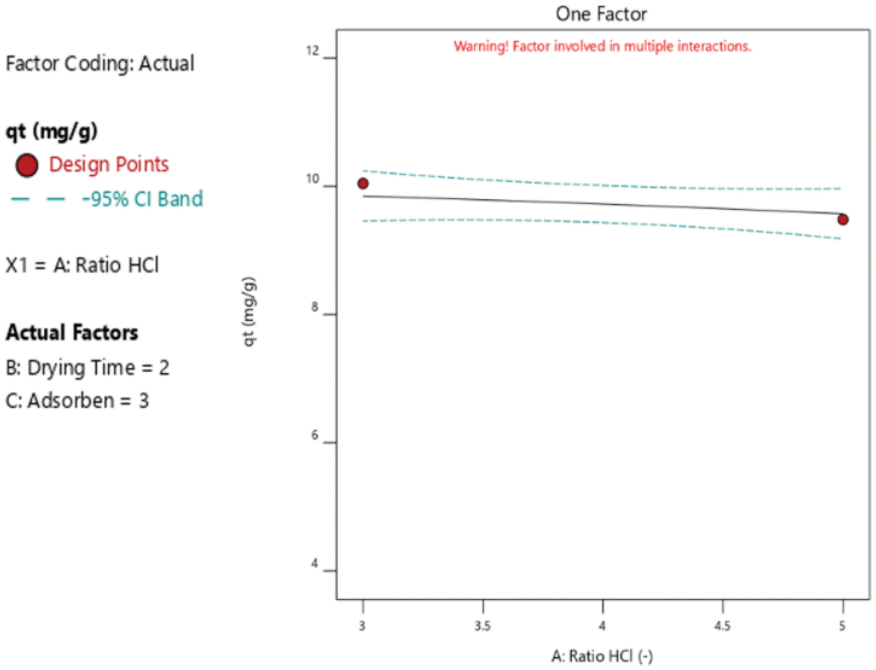

Fig. 7. Effect of the volume ratio of HCl versus q_t at 3%-w of adsorbent and drying time of 2 h.

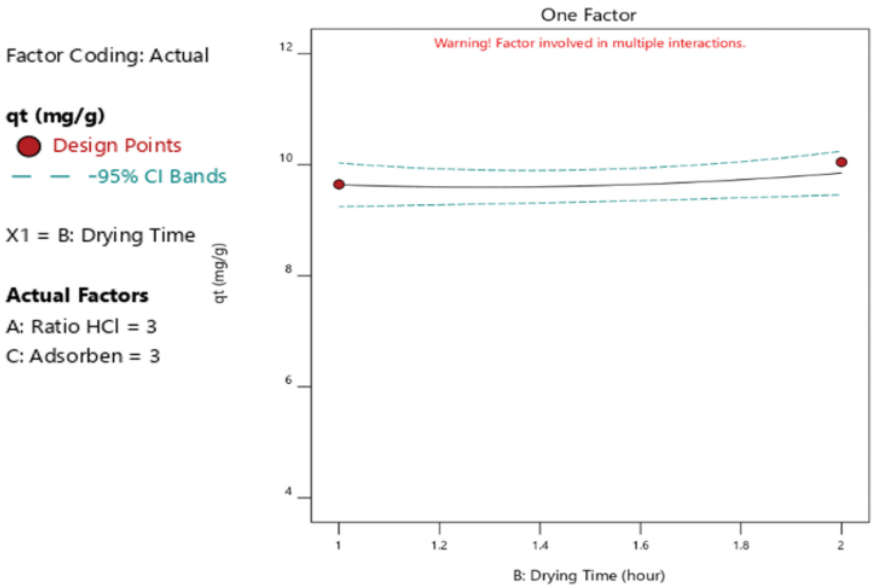

Fig. 8. Effect of drying time on q_t at 3%-w of adsorbent and ratio of HCl/sodium silicate of 3.

erol content in the untreated biodiesel at retention time of 50 min giving 0.46% area as DI-(9-Octadecenoyl-glycerin, while Fig. 11 prompts reduction of the glycerol content in the treated biodiesel releasing without any glycerin. It can be inferred that the silica

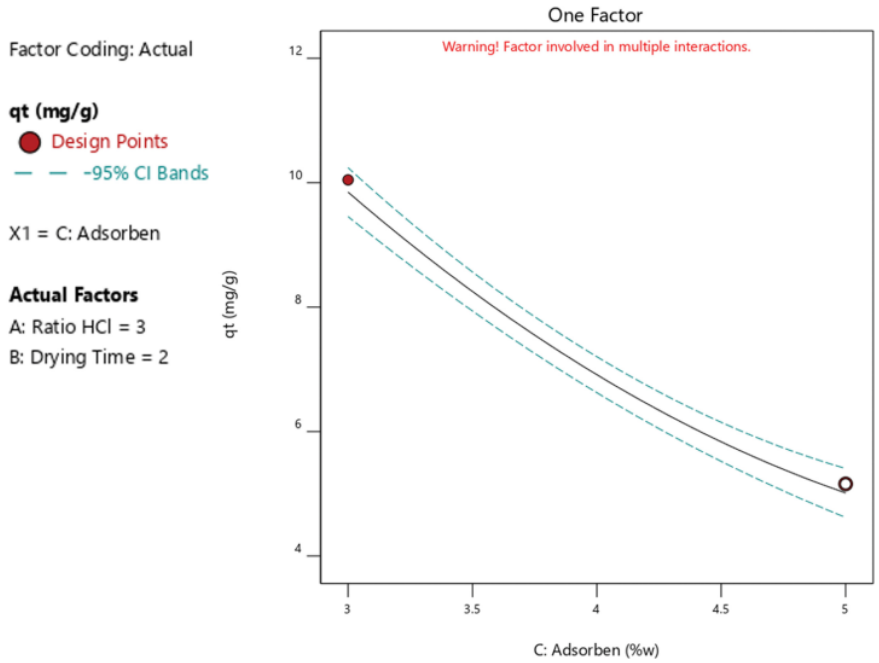

Fig. 9. Effect of adsorbent (in %-w) on q_t ratio of HCl/sodium silicate of 3 and drying time of 2 h.

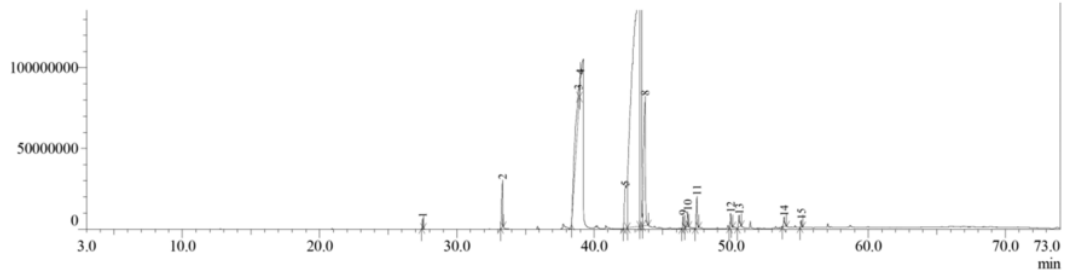

Peak Report TIC

Peak#	R.Time	Area	Area%	Height	Name
1	27.503	18319666	0.21	6188116	Dodecanoic acid, methyl ester (CAS)
2	33.332	149061168	1.68	29218876	Tetradecanoic acid, methyl ester (CAS)
3	38.870	471631508	5.32	13043228	Hexadecanoic acid, methyl ester (CAS)
4	39.005	29401555	0.33	3852658	Octadecanoic acid, 3-hydroxy-2-tetradecyl-, methyl ester (CAS)
5	42.280	331438947	3.74	25529476	9,12-Octadecadienoic acid (Z,Z)-, methyl ester (CAS)
6	43.160	5561269945	62.71	136664352	9,12-Octadecadienoic acid (Z,Z)-, methyl ester (CAS)
7	43.446	1288639123	14.53	147798615	9-Octadecenoic acid (Z)-, methyl ester (CAS)
8	43.733	718548925	8.10	80139413	Octadecanoic acid, methyl ester (CAS)
9	46.501	35191759	0.40	7605467	Hexadecanoic acid, 2-hydroxy-1,3-propanediyl ester (CAS)
10	46.835	34156185	0.39	9567076	11-Eicosenoic acid, methyl ester (CAS)
11	47.501	85694999	0.97	19126183	Eicosanoic acid, methyl ester (CAS)
12	49.966	40899552	0.46	8770424	DI-(9-OCTADECENOYL)-GLYCEROL
13	50.583	48271720	0.54	7261011	Hexadecanoic acid, 2-hydroxy-1-(hydroxymethyl)ethyl ester (CAS)
14	53.866	38272786	0.43	5912855	9-Octadecenoic acid (Z)-, 9-octadecenyl ester, (Z)- (CAS)
15	55.119	17852546	0.20	4359748	Tetracosanoic acid, methyl ester (CAS)
		8868650384	100.00	505037498	

Fig. 10. GCMS analysis on biodiesel.

adsorbent can adsorb the glycerol due to affinity of the silica regard with the existence of OH groups on the silica [78]. The organic compounds were also adsorbed on silica particles via hydrogen bonds forming between sylanol groups in the silica network and

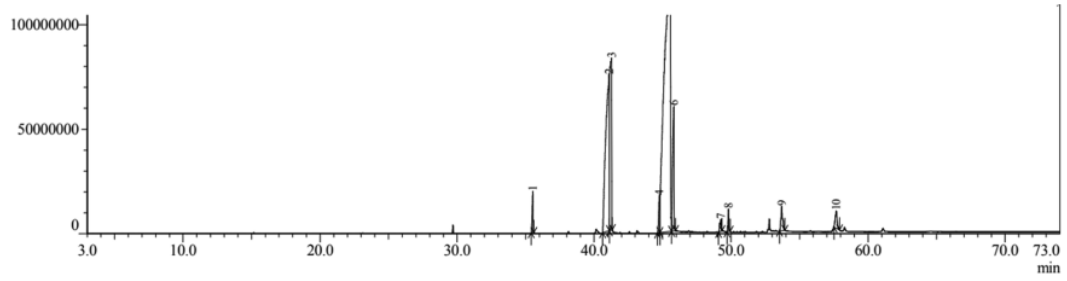

Peak Report TIC

Peak#	R.Time	Area	Area%	Height	Name
1	35.531	83686758	1.25	19668819	Tetradecanoic acid, methyl ester (CAS)
2	41.095	1337347311	19.99	74669052	Hexadecanoic acid, methyl ester (CAS)
3	41.270	762799178	11.40	82254527	Hexadecanoic acid, methyl ester (CAS)
4	44.760	111772316	1.67	17753686	9,12-Octadecadienoic acid (Z,Z)-, methyl ester (CAS)
5	45.567	3753030623	56.10	114335959	9-Octadecenoic acid (Z)-, methyl ester (CAS)
6	45.818	382198110	5.71	58255835	Octadecanoic acid, methyl ester (CAS)
7	49.253	37486144	0.56	5604450	11-Eicosenoic acid, methyl ester (CAS)
8	49.809	44294350	0.66	10717303	Eicosanoic acid, methyl ester (CAS)
9	53.698	99200658	1.48	11654475	Hexadecanoic acid, 2-hydroxy-1-(hydroxymethyl)ethyl ester (CAS)
10	57.672	78601070	1.17	8191201	9-Octadecenoic acid (Z)-, 2-hydroxy-1-(hydroxymethyl)ethyl ester (CAS)
		6690416518	100.00	403105307	

Fig. 11. GCMS analysis on treated biodiesel.

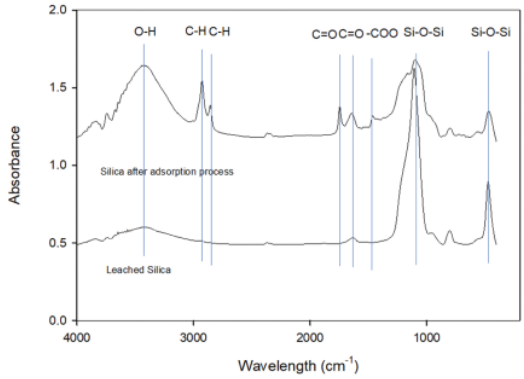

Fig. 12. FTIR analysis on silica after adsorption.

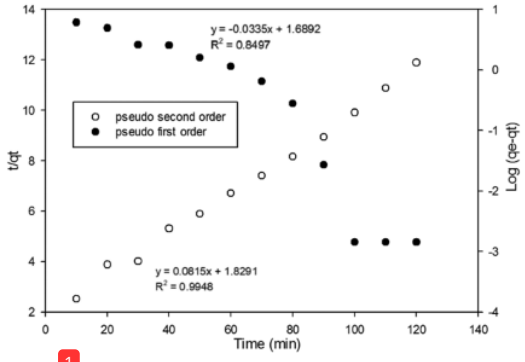

Fig. 13. Pseudo first order curve and pseudo second order curve.

hydroxyl-groups of the organic compounds [79]. Based on previous research [78], silica behaves as a non-selective adsorbent of high capacity that can adsorb different impurity types, which makes it an excellent adsorbent to purify biodiesel.

Fig. 12 displays the FTIR analysis of leached silica and the silica adsorbent after adsorption. The FTIR spectra shows the increase of the IR band at 3,400-3,420 cm^{-1} implies O-H stretching as the glycerol as well as a IR band of 1,739 cm^{-1} due to C=O stretching of the glycerol. The IR bands of 2,810-2,950 cm^{-1} and 1,655 cm^{-1} reflect as CH stretching and C=O from the glycerol, respectively [80]. The resulting silica shows affinity for glycerol in accordance with previous research [30]. The presence of glycerol was assigned to the IR band of 2,800 cm^{-1}-2,990 cm^{-1} and IR band of 1,675-1,500 cm^{-1} [81]. While, 1,400-1,460 cm^{-1} can be assigned to -COH bending corresponding as primary alcohol [82]. The appearance of the IR band at 465 cm^{-1} was due to the angular deformation of Si-O-Si [23]. The IR band of 1,093 cm^{-1} appeared from the stretching of the asymmetry of the Si-O-Si group [83]. However, the soap analysis was confirmed by using AOCS method Cc 17-79 to obtain soap in oil [65]. It was obtained that soap in untreated biodiesel attained (0.004±0.001) g soap/g sample, while the treated biodiesel earned no soap in sample. Even though, Fig. 12 does not occupy the existence of the IR band of soap significantly in silica used due to small amount of soap in untreated biodiesel. It was confirmed from previous research that a biodiesel refinery can be solved in one single stage using silica adsorbent by reducing impurities such as methanol residual, water, glycerin, free fatty acids, and soaps [78].

7. Kinetics Study

The adsorption rate constant can be obtained using kinetics studies by determination of glycerol content at certain time [84]. The kinetics studies provide demand of silica adsorbent to adsorb glycerol in certain amount of biodiesel at certain time. Determination of the adsorption rate constant requires the appropriate equation

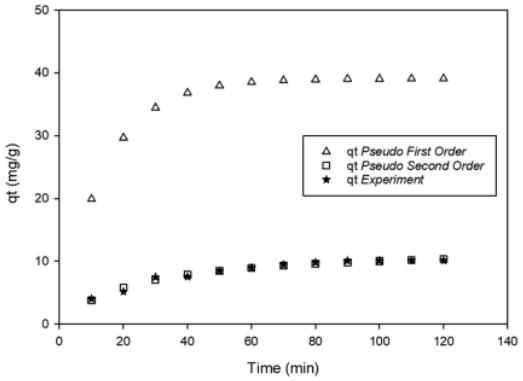

Fig. 14. Comparison of q_t experiment between pseudo first order q_t and pseudo second order.

model, such as pseudo-first-order and pseudo-second-order [16]. Fig. 13 shows curves of the pseudo-first-order and pseudo-second-order to obtain the adsorption rate constant (k). Table 6 shows the value of R^2 for both equation models.

Table 6 sums up the appropriate equation model with respect to pseudo-first- and second-order model. The regression value (R^2) of the pseudo-second-order closed to 1 and posed higher value of R^2 than that of the pseudo-first-order [85]. The pseudo-second-order can be properly used to describe the adsorption process in biodiesel purification according to other researches [35,54]. Fig. 14 reflects a comparison of the q_t value based on the pseudo-first-order and the pseudo-second-order with the experimental q_t value. It revealed that pseudo-second-order model met properly the experimental q_t value. Table 7 provides the comparison of the values of R^2, q_e, and k from previous and current studies. High q_e value indicates high adsorption capacity as well. The q_e value was obtained from this research of (10±0.02) mg/g and (39±0.01) mg/g for pseudo-second-order and pseudo-first-order, respectively. The q_e value is higher than the q_e value of the previous research [64]. The adsorption rate constant (k) of pseudo-second-order from this research (k=0.0036 g/mg.min) released lower than k value from previous research (k=0.0763 g/mg.min) [35,36,49]. The lower k value indicates the less glycerol adsorbed per gram of silica adsorbent at cer-

Tabel 6. Kinetics study

Equation model	Parameter	Value	
Pseudo-first-order	Equation	$\text{Log}(q_e - q_t) = -0.355\ t + 1.6892$	(8)
	k (1/min)	0.07715	
	R^2	0.8497	
Pseudo-second-order	Equation	$\frac{t}{q_t} = 0.0652\ t + 1.4633$	(9)
	k (g/mg·min)	0.0036	
	R^2	0.9948	

R^2: a measure of the amount of variation around the mean explained by the model
q_e: glycerol capacity adsorbed at equilibrium (mg/g)
q_t: glycerol capacity adsorbed at time t (mg/g)
k: adsorption rate constants

Table 7. Comparison of kinetics studies with previous research

Adsorbent type	Kinetics model						Reference
	Pseudo first order			Pseudo second order			
	k	q_e (mg/g) exp.	R^2	k	q_e (mg/g) exp.	R^2	
Chamotte clay	0.06 /min	1,326	0.97	0.00012 g /mg·min	1,326	0.99	[23]
Sugarcane bagasse	0.2311 /min	7.939	0.72	0.0763 g /mg·min	8.163	0.89	[64]
Activated carbon	0.0105 /min	0.281	0.89	0.000082 g /g·min	0.294	0.97	[66]
Silica aerogel	0.07712 /min	39±0.014	0.85	0.0036 g /mg·min	10±0.019	0.99	This research

R^2: a measure of the amount of variation around the mean explained by the model
k: adsorption rate constants
q_e: glycerol capacity adsorbed at equilibrium (mg/g)

tain time. While the adsorption rate constant (k) of pseudo-first-order released 0.0772/min in this research. Therefore, the silica aerogel adsorbent from the geothermal waste confirmed to retain a good performance based on the R^2, q_e, and k values in this research.

CONCLUSIONS

The lower HCl/sodium silicate ratio and the lower percent weight of adsorbent could increase the glycerin adsorption capacity in glycerol adsorption process in biodiesel using the silica derived from geothermal waste. Moreover, the longer drying time and larger surface area could increase the glycerol adsorption capacity. The silica was also confirmed by characterization of FTIR, BET, XRD, GPC, GCMS to prompt the adsorbent capability. The optimum condition of the silica preparation based on statistical analysis released with surface area of 371 m^2/g and glycerol adsorption capacity of (10±0.06)mg/g. This condition was attained at ratio volume of HCl to sodium silicate at 3, 2 hours of drying time at each temperature of 70 °C and 150 °C and 3%-w adsorbent of the silica. The kinetics study affirmed that the pseudo-second-order equation model can be used to describe the glycerin removal in biodiesel purification using the silica adsorbent.

ACKNOWLEDGEMENT

The authors received direct funding for this research from Directorate General of Higher Education Ministry of National Education Indonesia No. 257-68/UN7.6.1/PP/2020. The authors declare no conflict of interest.

LIST OF ACRONYMS AND ABBREVIATIONS

B : the required volume of hydrochloric acid in second titration of the soap analysis [mL]
C_o : glycerin concentration [mg/L]
C_e : glycerin concentration at equilibrium [mg/L]
GC : glycerin content [%]
h : hour
k_1 : adsorption rate constant in the pseudo-first order [1/min]
k_2 : adsorption rate constant in the pseudo-second order [g/mg·min]
N : normality
q_e : glycerin capacity adsorbed at equilibrium [mg/g]
q_t : glycerin capacity adsorbed at time t [mg/g]
rpm : revolutions per minute
R^2 : a measure of the amount of variation around the mean explained by the model
T_1 : volume of NaOH for sample titration [ml]
T_2 : volume of NaOH for blanks titration [ml]
V : volume of solution [mL]
W : sample weight [gr]
BET : Brunauer-Emmett-Teller
FTIR : Fourier Transform Infrared Spectroscopy
XRF : X-ray fluorescence
XRD : X-Ray Diffraction
SNI : Indonesian National Standard
GPC : Gel permeation chromatography
GCMS : Gas Chromatography Mass Spectrometry
NEP : National Energy Policy
ASTM: American Society for Testing and Materials
ANOVA : Analysis of Variance
RSME : Root Squared Mean Error

REFERENCES

1. M. Kumar and M. P. Sharma, *Renew. Sustain. Energy Rev.*, **56**, 1129 (2016).
2. S. Y. Pan, C. W. Li, Y. Z. Huang, C. Fan, Y. C. Tai and Y. L. Chen, *Bioresour. Technol.*, **318**, 124045 (2020).
3. K. L. Yu, W. H. Chen, H. K. Sheen, J. S. Chang, C. S. Lin, H. C. Ong, P. L. Show and T. C. Ling, *Fuel*, **279**, 118435 (2020).
4. A. S. Yusuff and J. O. Owolabi, *South African J. Chem. Eng.*, **30**, 42 (2019).
5. A. Jacob, B. Ashok, A. Alagumalai, O. H. Chyuan and P. T. K. Le, *Energy Convers. Manage.*, **228**, 113655 (2020).
6. J. Janaun and N. Ellis, *Renew. Sustain. Energy Rev.*, **14**, 1312 (2010).
7. J. Kansedo, K. T. Lee and S. Bhatia, *Biomass and Bioenergy*, **33**, 271 (2009).
8. A. Gashaw and A. Teshita, *Int. J. Renew. Sustain. Energy*, **3**, 92 (2014).
9. M. J. Yu, Y. B. Jo, S. G. Kim, Y. K. Lim, J. K. Jeon, S. H. Park, S. S. Kim and Y. K. Park, *Korean J. Chem. Eng.*, **28**, 2287 (2011).
10. J. H. Lee, S. B. Kim, H. Y. Yoo, J. H. Lee, S. O. Han, C. Park and S. W. Kim, *Korean J. Chem. Eng.*, **30**, 1335 (2013).
11. A. Avinash, P. Sasikumar and A. Pugazhendhi, *Renew. Sustain. Energy Rev.*, **134**, 110250 (2020).
12. A. Saravanakumar, A. Avinash and R. Saravanakumar, *Energy Sources, Part A Recover. Util. Environ. Eff.*, **38**, 2524 (2016).
13. M. Agarwal, G. Chauhan, S. P. Chaurasia and K. Singh, *J. Taiwan Inst. Chem. Eng.*, **43**, 89 (2012).
14. V. G. Tacias-Pascacio, B. Torrestiana-Sánchez, L. Dal Magro, J. J. Virgen-Ortíz, F. J. Suárez-Ruíz, R. C. Rodrigues and R. Fernandez-Lafuente, *Renew. Energy*, **135**, 1 (2019).
15. A. Avinash and A. Murugesan, *Sci. Rep.*, **7**, 1 (2017).
16. W. Pitakpoolsil and M. Hunsom, *J. Environ. Manage.*, **133**, 284 (2014).
17. L. R. Kumar, S. K. Yellapu and R. D. Tyagi, *Biodiesel production: technologies and future prospects*, R. D. Tyagi, R. Y. Surampalli, T. C. Zhang, S. Yan and X. Zhang Eds., American Society of Civil Engineers, Washington (2019).
18. M. L. Pisarello, B. O. D. Costa, N. S. Veizaga and C. A. Querini. *Ind. Eng. Chem. Res.*, **49**, 8935 (2010).
19. C. S. Faccini, M. E. Da Cunha, M. S. A. Moraes, L. C. Krause, M. C. Manique, M. R. A. Rodrigues, E. V. Benvenutti and E. B. Caramão, *J. Braz. Chem. Soc.*, **22**, 558 (2011).
20. M. C. P. Cruz, S. P. Ravagnani, F. M. S. Brogna, S. P. Campana, G. C. Triviño, A. C. L. Lisboa and L. H. I. Mei, *Biotechnol. Appl. Biochem.*, **40**, 243 (2004).
21. M. Berrios and R. L. Skelton, *Chem. Eng. J.*, **144**, 459 (2008).
22. M. C. Manique, C. S. Faccini, B. Onorevoli, E. V. Benvenutti and E. B. Caramão, *Fuel*, **92**, 56 (2012).
23. F. D. Santos, L. R. V. da Conceição, A. Ceron and H. F. de Castro,

Appl. Clay Sci., **149**, 41 (2017).
24. M. G. Gomes, D. Q. Santos, L. C. De Morais, and D. Pasquini, *Fuel*, **155**, 1 (2015).
25. A. L. Squissato, D. M. Fernandes, R. M. F. Sousa, R. R. Cunha, D. S. Serqueira, E. M. Richter, D. Pasquini and R. A. A. Muñoz, *Cellulose*, **22**, 1263 (2015).
26. M. Catarino, E. Ferreira, A. P. S. Dias and J. Gomes, *Chem. Eng. J.*, **396**, 123930 (2020).
27. F. D. Santos, L. Rafael, V. Conceição, D. S. Giordani and H. F. De Castro, *Int. J. Eng. Res. Sci.*, **2**, 34 (2016).
28. J. C. Yori, S. A. D'Ippolito, C. L. Pieck and C. R. Vera, *Energy Fuels*, **21**, 347 (2007).
29. Z. J. Predojević, *Fuel*, **87**, 3522 (2008).
30. V. A. Mazzieri, C. R. Vera and J. C. Yori, *Energy Fuels*, **22**, 4281 (2008).
31. M. Ahmaruzzaman and V. K. Gupta, *Ind. Eng. Chem. Res.*, **50**, 13589 (2011).
32. A. Purnomo, F. Dalanta, A. D. Oktaviani and S. Silviana, *AIP Conf. Proc.*, **2026**, 020077 (2018).
33. S. Silviana, A. Noorpasha and M. M. Rahman, *Civ. Eng. Archit.*, **8**, 281 (2020).
34. S. Silviana, A. Darmawan, A. A. Janitra, A. Ma'ruf and I. Triesty, *Int. J. Emerg. Trends Eng. Res.*, **8**, 4854 (2020).
35. D. Musino, *Impact of surface modification on the structure and dynamics of silica-polymer nanocomposites*, PhD diss., Université Montpellier (2018).
36. A. M. Alswieleh, *J. Chem.*, **2020**, 1 (2020).
37. K. Sarikhani, K. Jeddi, R. B. Thompson, C. B. Park and P. Chen, *Langmuir*, **31**, 5571 (2015).
38. H. K. D. Nguyen, P. T. Hoang and N. T. Dinh, *J. Braz. Chem. Soc.*, **29**, 1714 (2018).
39. N. Pal and A. Mandal, *Chem. Eng. Sci.*, **226**, 115887 (2020).
40. N. Saengprachum and S. Pengprecha, *Int. Conf. Life Sci. Eng.*, **45**, 1[illegible]2012).
41. S. R. da Silva, N. J. A. de Albuquerque, R. M. de Almeida and F. C. de Abreu, *Materials* (Basel), **10**, 1132 (2017).
42. S. L. Raja, *J. Chem. Nat. Resour.*, **1**, 88 (2019).
43. G. G. Kaya and H. Deveci, *J. Ind. Eng. Chem.*, **89**, 13 (2020).
44. M. L. N. Perdigoto, R. C. Martins, N. Rocha, M. J. Quina, L. Gando-Ferreira, R. Patrício and L. Durães, *J. Colloid Interface Sci.*, **380**, 134 (2012).
45. J. H. Moon, H. Ahn, S. H. Hyun and C. H. Lee, *Korean J. Chem. Eng.*, **21**, 477 (2004).
46. J. Ryu, S. M. Kim, J. W. Choi, J. M. Ha, D. J. Ahn, D. J. Suh and Y. W. Suh, *Catal. Commun.*, **29**, 40 (2012).
47. J. L. Gurav, I. K. Jung, H. H. Park, E. S. Kang and D. Y. Nadargi, *J. Nanomater.*, **2010**, 1 (2010).
48. S. Motahari, M. Nodeh and K. Maghsoudi, *Desalin. Water Treat.*, **57**, 16886 (2016).
49. C. Li, J. Zhu, M. Zhou, S. Zhang and X. He, *Materials* (Basel), **12**, 1782 (2019).
50. H. Y. Nah, V. G. Parale, H. N. R. Jung, K. Y. Lee, C. H. Lim, Y. S. Ku and H. H. Park, *J. Sol-Gel Sci. Technol.*, **85**, 302 (2018).
51. A. V. Rao, M. M. Kulkarni, D. P. Amalnerkar and T. Seth, *Appl. Surf. Sci.*, **206**, 262 (2003).
52. M. Zabeti, W. M. A. W. Daud and M. K. Aroua, *Fuel Process. Technol.*, **91**, 243 (2010).
53. U. K. H. Bangi, A. V. Rao and A. P. Rao, *Sci. Technol. Adv. Mater.*, **9**, 035006 (2008).
54. J. Li, C. Wan, Y. Lu and Q. Sun, *Front. Agric. Sci. Eng.*, **1**, 46 (2014).
55. N. A. Pambudi, R. Itoi, R. Yamashiro, B. Y. C. S. Alam, L. Tusara, S. Jalilinasrabady and J. Khasani, *Geothermics*, **54**, 109 (2015).
56. S. Silviana, R. M. Hasbi, C. P. Sagita, O. D. Nurhayati, A. Fauzan, S. Suhartana and J. U. D. Hatmoko, *Proceeding of Seminar Teknologi Hijau 2*, **1**, 341 (2017).
57. S. Silviana, G. J. Sanyoto, A. Darmawan and H. Sutanto, *Rasayan J. Chem.*, **13**, 1692 (2020).
58. S. Silviana, I. N. H. Rambe, H. Sudrajat and M. A. Zidan, *AIP Conf. Proc.*, **2202**, 020069 (2019).
59. S. Silviana, A. Darmawan, A. Subagio and F. Dalanta, *ASEAN J. Chem. Eng.*, **19**, 91 (2019).
60. S. Silviana, A. Darmawan, F. Dalanta, A. Subagio, F. Hermawan and H. M. Santoso, *Materials (Basel)*, **14**, 1 (2021).
61. S. Affandi, H. Setyawan, S. Winardi, A. Purwanto and R. Balgis, *Adv. Powder Technol.*, **20**, 468 (2009).
62. S. E. Lee, Y. S. Ahn, J. S. Lee, C. H. Cho, C. K. Hong and O. H. Kwon, *J. Ceram. Process. Res.*, **18**, 777 (2017).
63. F. Furqon, A. K. Nugroho and M. K. Anshorulloh, *Rona Tek. Pertan.*, **12**, 22 (2019).
64. M. J. Alves, Í. V. Cavalcanti, M. M. de Resende, V. L. Cardoso and M. H. Reis, *Ind. Crops Prod.*, **89**, 119 (2016).
65. J. Van Gerpen, B. Shanks, R. Pruszko, D. Clements and G. Knothe, *Biodiesel analytical methods: August 2002-January 2004*, National Renewable Energy Lab., United States (2004).
66. É. De Castro Vasques, C. R. G. Tavares, C. I. Yamamoto, M. R. Mafra and L. Igarashi-Mafra, *Environ. Technol.*, (United Kingdom), **34**, 2361 (2013).
67. M. A. Azmi, N. A. A. Ismail, M. Rizamarhaiza, A. A. K. W. M. Hasif and H. Taib, *AIP Conf. Proc.*, **1756**, 020005 (2016).
68. S. Musić, N. Filipović-Vinceković and L. Sekovanić, *Brazilian J. Chem. Eng.*, **28**, 89 (2011).
69. A. M. Anderson and M. K. Carroll, in *Aerogels handbook*, M. A. Aegerter, N. Leventis, M. M. Koebel Eds., Adv. Sol-Gel Deriv. Materials Technol., New York (2011).
70. H. Tamon, T. Kitamura and M. Okazaki, *J. Colloid Interface Sci.*, **197**, 353 (1998).
71. M. Lazrag, C. Lemaitre, C. Castel, A. Hannachi and D. Barth, *J. Supercrit. Fluids*, **140**, 394 (2018).
72. J. Bajorath, *Chemoinformatics: Concepts, methods, and tools for drug discovery*, Humana Press, New Jersey (2004).
73. V. Apostolopoulou-Kalkavoura, P. Munier and L. Bergström, *Adv. Mater.*, **2001839**, 1 (2020).
74. M. A. Ashraf, W. Peng, Y. Zare and K. Y. Rhee, *Nanoscale Res. Lett.*, **13**, 1 (2018).
75. S. H. Soytaş, O. Oğuz and Y. Z. Menceloğlu, in *Polymer composites with functionalized nanoparticles*, K. Pielichowski and T. M. Majka Eds., Elsevier (2018).
76. S. Karamikamkar, H. E. Naguib and C. B. Park, *Adv. Colloid Interface Sci.*, **276**, 102101 (2020).
77. C. Jeon and H. P. Kwang, *Water Res.*, **39**, 3938 (2005).
78. D. L. Manuale, E. Greco, A. Clementz, G. C. Torres, C. R. Vera and J. C. Yori, *Chem. Eng. J.*, **256**, 372 (2014).

79. L. S. Martin, A. Ceron, P. C. Oliveira, G. M. Zanin and H. F. de Castro, *J. Ind. Eng. Chem.*, **62**, 462 (2018).
80. M. Danish, M. W. Mumtaz, M. Fakhar and U. Rashid, *Chiang Mai J. Sci.*, **44**, 1570 (2017).
81. M. P. Fuller, G. L. Ritter and C. S. Draper, *Appl. Spectrosc.*, **42**, 217 (1988).
82. S. Kongjao, S. Damronglerd and M. Hunsom, *Korean J. Chem. Eng.*, **27**, 944 (2010).
83. B. H. Stuart, *Infrared spectroscopy: Fundamentals and applications*, John Wiley & Sons, Ltd, Chichester (2005).
84. I. Raheem, M. N. Bin Mohiddin, Y. H. Tan, J. Kansedo, N. M. Mubarak, M. O. Abdullah and M. L. Ibrahim, *J. Ind. Eng. Chem.*, **91**, 54 (2020).
85. V. Chairgulprasert and P. Madlah, *Sci. Technol. Asia*, **23**, 1 (2018).

Utilization of geothermal waste as a silica adsorbent for biodiesel purification

ORIGINALITY REPORT

4%	4%	3%	1%
SIMILARITY INDEX	INTERNET SOURCES	PUBLICATIONS	STUDENT PAPERS

PRIMARY SOURCES

1	dns2.asia.edu.tw Internet Source	1%
2	Le Zhang, Kai-Chee Loh, Agnès Kuroki, Yanjun Dai, Yen Wah Tong. "Microbial biodiesel production from industrial organic wastes by oleaginous microorganisms: Current status and prospects", Journal of Hazardous Materials, 2021 Publication	1%
3	Flavia D. Santos, Leyvison Rafael V. da Conceição, Annie Ceron, Heizir F. de Castro. "Chamotte clay as potential low cost adsorbent to be used in the palm kernel biodiesel purification", Applied Clay Science, 2017 Publication	1%
4	idoc.pub Internet Source	1%
5	Lucas S. Martin, Annie Ceron, Pedro C. Oliveira, Gisella M. Zanin, Heizir F. de Castro.	1%

"Different organic components on silica hybrid matrices modulate the lipase inhibition by the glycerol formed in continuous transesterification reactions", Journal of Industrial and Engineering Chemistry, 2018

Publication

Exclude quotes	On	Exclude matches	< 1%
Exclude bibliography	Off		

Utilization of geothermal waste as a silica adsorbent for biodiesel purification

GRADEMARK REPORT

FINAL GRADE

/0

GENERAL COMMENTS

Instructor

PAGE 1

PAGE 2

PAGE 3

PAGE 4

PAGE 5

PAGE 6

PAGE 7

PAGE 8

PAGE 9

PAGE 10

PAGE 11

PAGE 12

PAGE 13

PAGE 14

PAGE 15